

Joint simulation method for ultra-wideband electromagnetic pulse irradiation effect on a certain type of anti-tank missile fuze

Rong He ¹, Chenyang Zhang ¹, Shuai Chen ¹ and Xiangjin Zhang ¹

¹ School of mechanical Engineering, Nanjing University of Science and Technology, Nanjing 290014, China;

Abstract. Taking a certain type of anti-tank missile all-electronic safety system as the research object, based on the existing fuse model and circuit, using different simulation software to establish the excitation source and device model that meets the requirements, and using the joint simulation method to establish a complete simulation system from 'field' to 'device' for the effect of the ultra-wideband electromagnetic pulse. Using the joint simulation method, a complete simulation system from 'field' to 'device' is established for the ultra-wideband electromagnetic pulse effect. The field strength of the external interference source in the battlefield environment is analyzed, and the field strength radiated in the cavity through the coupling path. The establishment of the semiconductor device electro-thermal simulation model, the study of the electromagnetic pulse injection on the internal sensitive devices caused by the loss mechanism and the cause of failure, the use of the joint simulation method in a comprehensive assessment of a certain type of anti-tank missile fuzes in the ultra-broadband electromagnetic pulse irradiation capacity at the same time, but also accurately understand the fuse system in the most susceptible to the impact of the ultra-broadband electromagnetic pulse in the part of the protective measures to provide guidance.

Keywords: Ultra-wideband EMP; PMOS; Negative Bias Temperature Instability.

1. Introduction

In order to improve the reliability and safety of the all-electronic safety system in anti-tank missiles, the electromagnetic radiation interference problem becomes the primary factor to be considered, and the research and design of electromagnetic protection measures for anti-tank missile fuzes become crucial. In particular, the ultra-wideband (UWB) strong electromagnetic pulse has a very short rise time, high peak power, and rich spectral components, which can damage and interfere with the target electronic system through the 'front door' or 'back door' coupling effect, and is more likely to have an impact on the normal operation of the fuse [1].

The mechanism of ultra-wideband irradiation effect of the fuse is the premise of protection and reinforcement technology research, Zhang Wei et al. established a microstrip line SPICE circuit model under the external field incidence, two-dimensional semiconductor device-circuit simulation program combined with the simulation and analysis of PCB circuit system in the high-power microwave (HPM) under the irradiation effect, but the lack of analysis on the damage effect of the specific internal devices [2]. Zheng Fuquan et al. used CST software to establish a strong electromagnetic pulse coupling simulation model to obtain the distribution of electric field inside and outside the artillery fuse. The electronic system directly irradiation test, the test results show that the shell of the fuse to the external field strength is not greater than 45kV/m, the electronic system has a certain protective effect [3], but more than 50kV/m ultra-broadband high-power microwave source on the fuse inside the electronic system damage effect is not yet known. Korte et al. in Germany conducted a sensitivity threshold study for TTL and COMS inverters under the action of ultra-wideband signals (UWB) and electromagnetic pulse signals (EMP), which showed that transistor damage was caused by triggering the transmitter junction to penetrate under the condition of low E-field strength (540 kV/m); interconnections in the integrated circuits were melted when the E-field strength increased to 720 kV/m; and the interconnections in the integrated circuits melted when the E-field strength increased again [4]. Summarising the above literature, most of the studies on the irradiation effect of ultra-wideband electromagnetic pulse on fuses are

based on experiments, but the manufacturing cost of fuses is high, and the cost of experiments is high, so how to use simulation software to establish a complete simulation system on the basis of existing fuses to counterpropagate the influence of fuses by ultra-wideband electromagnetic pulse is an urgent problem to be solved nowadays.

Therefore, this paper takes a certain type of anti-tank missile all-electronic safety system as the research object, using different simulation software to establish the excitation source, device model that meets the requirements, using the joint simulation method, the electrical and thermal effects of the ultra-wideband electromagnetic pulse to establish a ‘field’ to ‘device’ from the ‘field’ to the ‘field’ of the ‘device’. A complete simulation system from ‘field’ to ‘device’ is established for the electric and thermal effects of ultra-wideband electromagnetic pulse using the joint simulation method. The field strength of the external interference source in the battlefield environment is analysed, which is radiated in the cavity through the coupling path. The establishment of semiconductor device electrical and thermal simulation model, the study of electromagnetic pulse injection on the internal sensitive devices caused by the loss mechanism and failure causes, the use of the joint simulation method in a comprehensive assessment of a certain type of anti-tank missile fuzes in the ultra-broadband electromagnetic pulse irradiation capacity at the same time, but also accurately understand the fuzing system in the most susceptible to the influence of the ultra-broadband electromagnetic pulse in the part of the protective measures to provide guidance.

2. Modelling of ultra-wideband electromagnetic pulse (UWB) interference sources

Ultra Wide Band (UWB) pulses are typical and widely used broadband signals with small pulse widths, large bandwidths, often with a percentage bandwidth of more than 25%, short rising edges of only a few nanoseconds, and frequencies in the range of 100MHz to 50GHz [5]. where the percentage bandwidth pbw of the signal is defined in Equation 1.

$$pbw = \frac{2(f_H - f_L)}{(f_H + f_L)} \times 100\% \quad (1)$$

Where f_H is the upper limit frequency of the energy bandwidth frequency range and f_L is the lower limit frequency of the energy bandwidth. The energy bandwidth is the frequency range that contains more than 90% of the signal energy. The percentage bandwidth of UWBs used today has reached 180%, which can cover a wide range of target system operating frequencies with high energy, which is a very significant threat to electronic equipment. Pulse forms such as Gaussian, bipolar, biexponential and Elmitic pulses are often used to describe ultra-wideband high power microwaves, with Gaussian pulses being the most widely used. In this paper, Gaussian pulse modulated UWB is used as an EMP source, and its expression is shown in equation 2.

$$E(t) = E_0 \exp\left(\frac{-4\pi(t - t_d)^2}{t_w^2}\right) \quad (2)$$

Where $E(t)$ is the field strength of the incident Gaussian pulse in the time domain, E_0 is the peak field strength of the UWB pulse, t_d is the moment of the pulse peak appearance, and t_w pulse width. In this paper, $E_0=50\text{kV/m}$, $t_d=1.2\text{ns}$, $t_w=0.95\text{ns}$ are chosen, and the corresponding waveforms are shown in Fig. 1. The Fourier transform of Eq. 3 yields the frequency domain field strength $E(\omega)$.

$$\begin{aligned} E(\omega) &= \int_{-\infty}^{+\infty} E(t)e^{-i\omega t} dt \\ &= \int_{-\infty}^{+\infty} E_0 e^{\frac{-4\pi(t-t_d)^2}{t_w^2}} e^{-i\omega t} dt \end{aligned} \quad (3)$$

Let $u = t - t_d$, $\alpha = 4\pi/t_w^2$.

$$\begin{aligned}
 E(\omega) &= E_0 e^{-i\omega t_d} \int_{-\infty}^{+\infty} e^{-\alpha u^2} e^{-i\omega u} du \\
 &= \frac{E_0 t_w}{2} e^{-\left(\frac{\omega^2 t_w^2}{16\pi} + i\omega t_d\right)}
 \end{aligned}
 \tag{4}$$

The transformed frequency domain curves are shown in Fig. 2, which shows that the spectrogram of the Gaussian pulse used is still Gaussian and the energy distribution is mainly in the range of 0 to 5 GHz.

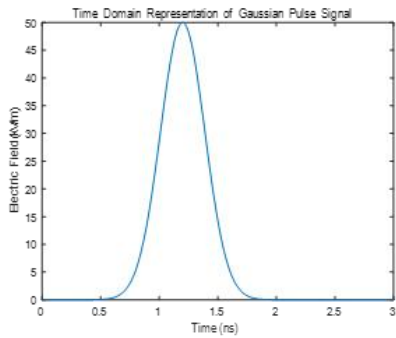


Fig. 1 UWB time domain signal waveform

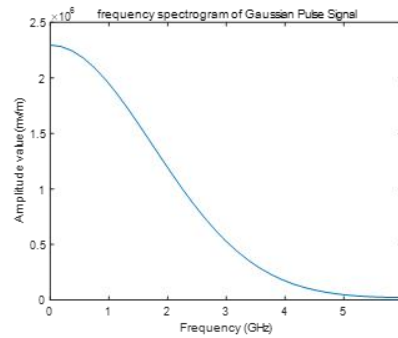


Fig. 2 UWB frequency domain signal waveform

In the closed cavity, the shell and the fuze shell can effectively shield the external electromagnetic wave, thus protecting the internal electronic components. When subjected to ultra-wideband (UWB) pulses, the electric field strength at the geometric centre of the fuze cavity varies with time as shown in Fig. After adding coils and connecting lines, the electric field amplitude at the geometrical centre of the cavity is increased to 89 V/m, which is 54 dB lower compared to the electric field source. under the influence of these connections, the electromagnetic energy outside the cavity is coupled into the device cavity through the coils, which results in a significant enhancement of the electric field inside the cavity. Under the effect of UWB interference, the electric field strength inside the fuzed cavity reaches 89 V/m, and the electromagnetic energy coupled into the cavity is mainly concentrated in the high frequency band, which may cause serious damage to the electronic equipment inside the cavity.

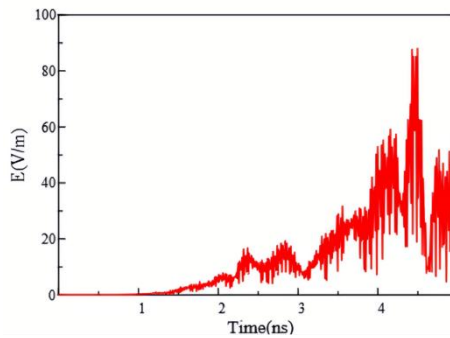


Fig. 3 Electric field strength in the fuzing cavity in the presence of UWB interference

3. Electromagnetic field coupling strength analysis

Electromagnetic radiation through the coupling path into the missile cavity of electromagnetic energy will ultimately act in the form of antenna coupling at the ends of the electronic equipment to form an induced voltage or current, and on the sensitive devices in the line to cause the impact, especially in the modern new EMP jamming bomb under the irradiation of the coupling of the large voltage or even directly caused by the line or the device's serious burned out. To study the failure mode of semiconductor devices in electromagnetic interference also need to analyse the electric field strength coupled in the cable voltage size.



Fig. 4 Typical Equivalent Circuit

Fuse circuit on the PCB was ring-shaped distribution and size is much smaller than the wavelength of electromagnetic radiation, can be regarded as a small loop antenna, see Figure 4. its acceptance of external radiation into the antenna ends of the voltage V to be calculated by the formula 5

$$V = FE \tag{5}$$

Where, E shows the electric field strength in the fusing environment, F is the antenna coefficient, which is affected by the antenna size, material and other characteristics. F Can be calculated by equation 6

$$F = \frac{h_e}{\frac{Z_e + Z_l}{Z_l}} \tag{6}$$

where Z_e denotes the antenna effective impedance, which is determined by the antenna material, Z_l denotes the load effective impedance, and h_e shows the antenna height. It is used to indicate the relationship between the antenna incoming field strength size and the induced coupling voltage generated, which can be calculated by equation 7

$$h_e = \frac{Z_e + Z_l}{Z_l} \sqrt{\frac{S_{max} R_r}{Z_w}} \tag{7}$$

S_{max} represents the effective receiving area of the antenna, which is affected by the size of the antenna loop, Z_w represents the wave impedance, and R_r represents the radiation resistance. S_{max} can be expressed in terms of wavelength Z_w antenna gain G as

$$S_{max} = \frac{G \lambda^2}{\pi} \tag{8}$$

According to the impedance matching requirements can be set $Z_e = Z_l = R_r = 50 \Omega$. Since the electromagnetic radiation is directly coupled from the air into the antenna, then the query information can be obtained $Z_w = 377 \Omega$. Then the formula 7 can be written as

$$h_e = \frac{\lambda \sqrt{G}}{2.43} \tag{9}$$

The value of gain G in Eq. needs to be based on the antenna's directivity coefficient (direction versus irradiated power direction) $D(\theta, \varphi)$ and the antenna's coupling efficiency η see Eq.

$$G = D(\theta, \varphi) \cdot \eta \tag{10}$$

Where θ and φ respectively represent the irradiated power and the base axis y-axis and z-axis direction angle, can be by the direction of the antenna's radiated power and no antenna radiated power of the ratio, see equation

$$D(\theta, \varphi) = \frac{P_r(\theta, \varphi)}{P_r} \tag{11}$$

And η shows the ratio of the antenna's radiated power P_r to the radiated input power P_{in}

$$\eta = \frac{P_r}{P_{in}} = \frac{P_r}{P_r + P_d} \tag{12}$$

Where P_d denotes the antenna loss power, for the loop microstrip antenna, after reviewing the information, usually defaults to its antenna efficiency is about 1. Getting G , according to the UWB frequency domain characteristics, it can be obtained as

$$V = \frac{\lambda \sqrt{G}}{4.87} \cdot E = 37V \tag{13}$$

According to the calculation, the voltage of UWB coupling in the circuit is 37 V. Then the damage mechanism and destruction threshold of power semiconductor sensitive devices are analysed.

4. Failure mechanism of PMOS tubes under ultra-wideband electromagnetic pulse interference

Electromagnetic field energy coupling into the electronic system, so that the device level flip, performance degradation or even burned resulting in abnormal system operation phenomenon is known as the EMP effect [6], and prone to EMP effect of the semiconductor device is known as sensitive devices. All-electronic safety system in the safety and logic control deactivation module is responsible for controlling the power-up, deactivation and overload and other parameters to complete the process of boosting the detonation, it can be said that the control module can work properly with the fuse is directly related to whether or not the normal role. In the control module, two static switches and a dynamic switch is a key electronic components, often using MOS tubes, IGBT tubes and other power semiconductor switching devices to facilitate the control of the voltage on and off. A type of anti-tank missile fuzes all-electronic safety system design static switch 1 using PMOS tube, because its gate is a high impedance terminal, if the gate is suspended, MOS tube may be due to accidental interference with the conductor, so the gate needs to be connected to the ground resistance, and the PMOS tube is usually the existence of parasitic diodes to prevent the source and drain reverse connection. Pmos tubes are electromagnetically sensitive devices in the control module.

4.1 PMOS Device Simulation

Firstly, Athena is used to mesh the structure model and define the PN junction position after dividing the area. After the construction is completed, use save to save the structure file, and then use Atlas to set the excitation signal, calculation method and contact mode definition, the simulation is intended to simulate the normal operation of the transistor is subjected to the damage generated by the electromagnetic pulse, so the boundary conditions are used for ohmic contact, the metal material aluminium is used as the electrode, so as to make the transistor and the external form a good ohmic contact, and the heat can only be achieved through the metal contact to achieve the circulation of heat, and the rest of the device is set as adiabatic [7]. The rest of the device is set to be adiabatic. Finally, the obtained diagrams of the internal physical quantities and characteristic parameters of the device are analysed to study the loss pattern of the PMOS tube by EMP.

In this paper, the transistor is studied and analysed using Silvaco TCAD software to build a 2D simulation model of the PMOS device as shown in Fig. 1. In the STI oxide layer and channel interface and channel and Si/SiO₂: interface to set the refinement of the grid, the grid size of 1 nm, the rest of the 20 nm, in order to improve the simulation computing rate, set the number of grids does not exceed the software's upper limit of 2000. through the continuous optimization and adjustment of the device model in the simulation as far as possible with the real device, so as to improve the credibility of the simulation. The model is a typical PMOS tube structure, P-N-P structure, the model lateral width for the type of lateral width of 1 μm, the junction depth of 0.15 μm, the figure of the base (abstract) and the source (source) grounded, the gate (gate) external voltage source, the drain (drain) injected into the electromagnetic pulse signal, the completion of the modelling of the silicon (Si) as the substrate for ion implantation and diffusion, the substrate for the P-N-P structure, the model is a typical PMOS tube structure. and diffusion, P-type doping of the substrate, doped phosphorus (phos) concentration of $1.0 \times 10^{17}/\text{cm}^3$, followed by N-well generation, doped boron difluoride (bf2) concentration of $9.0 \times 10^{12}/\text{cm}^3$, the use of a Gaussian distribution, the source and drain P-type doping to generate a P-well, the concentration of boron difluoride (bf2) is $1.5 \times 10^{15}/\text{cm}^3$, the source and the drain between the is an N-type semiconductor. The concentration distribution in the realised tube is shown in Fig. 4.

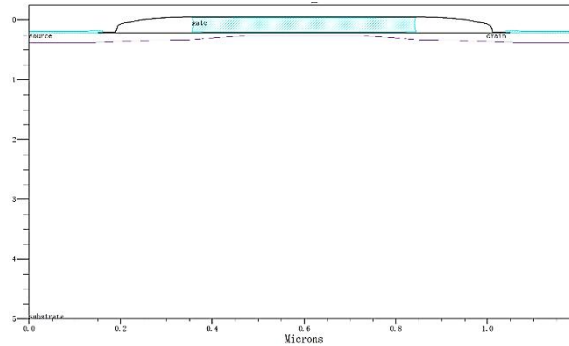


Fig. 5 PMOS tube two-dimensional structure diagram

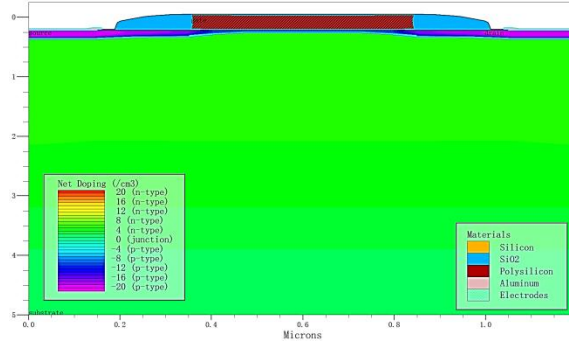


Fig. 6 Doping concentration distribution

According to the PMOS device model, the simulation is simulated to obtain the linear transfer characteristic curve of the PMOS device. As can be seen from Figure 2, the tube conducts when the device voltage is greater than -0.9 V , there is drain current, that is, the turn-on voltage of the tube is -0.9 V . This curve is basically consistent with the transfer curve of the actual PMOS device test, proving that the PMOS device model established in this paper can simulate the simulation of the actual device.

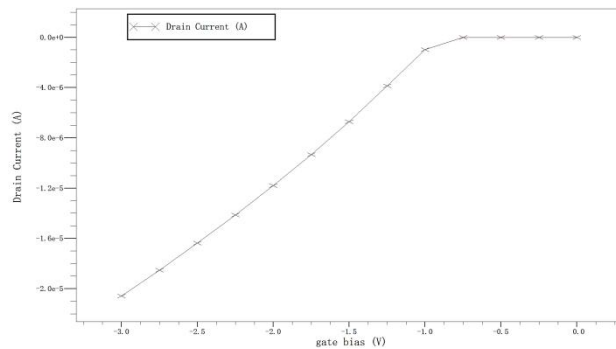


Fig. 7 Linear transfer characteristics of 30 am PMOS devices

4.2 Simulation results and data analysis

Negative Bias Temperature Instability (NBTI) is a phenomenon that occurs when the PMOS operates with negative gate voltage and higher temperatures, and the device parameters NBTI is a phenomenon of PMOS device parameter degradation when operating at negative gate voltage and higher temperature, which is manifested by the decreasing absolute value of PMOS leakage current I_d and transconductance G_{max} , and the increasing absolute value of threshold voltage V_{th} . In timing circuits, the NBTI effect increases the signal delay and leads to timing drift; in analogue circuits, especially in analogue circuits with high parameter matching requirements, the NBTI effect can lead to device mismatches that reduce the accuracy of the circuits or even prevent them from working properly [8]. Therefore, it is very important to study the impact of NBTI effect on the high performance and high reliability design of integrated circuits.

Using the PMOS tube device model described above, a negative bias temperature instability model is established, the traps are initialised as all being in the precursor state, and then transient

simulations are carried out under negative gate bias, with the device biased to on. The transient electrical characteristics of the stressed and relaxed states at high temperatures are simulated.

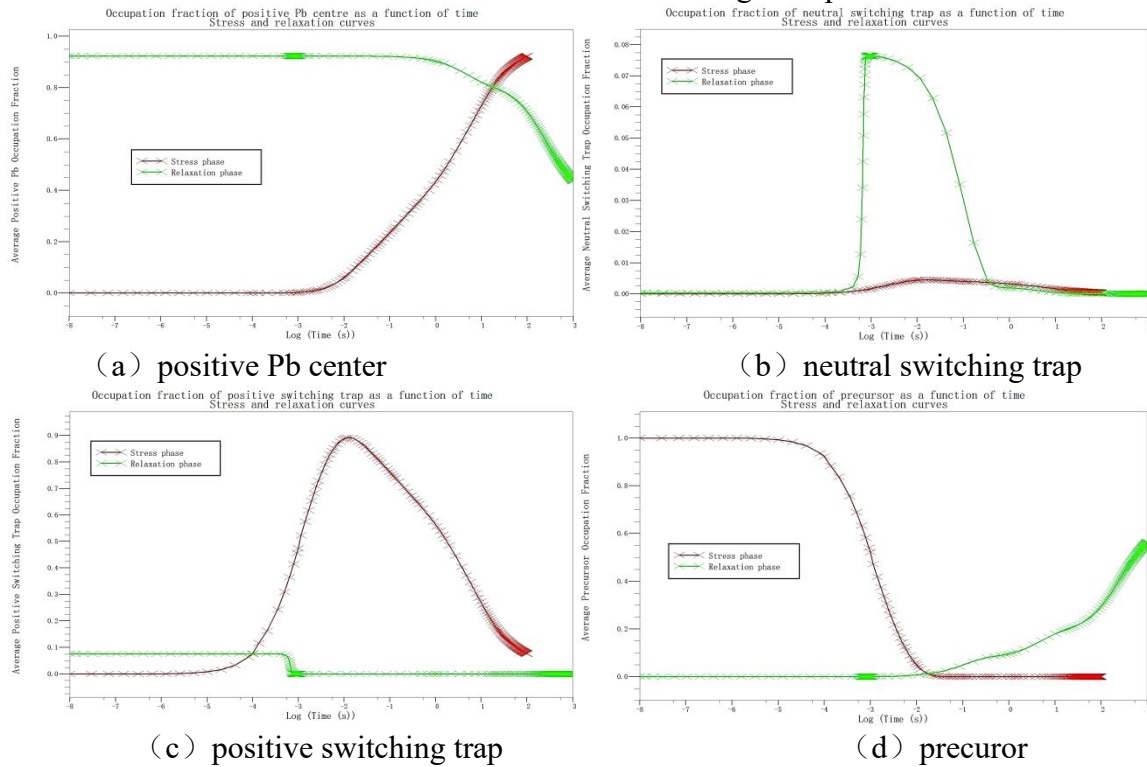


Fig. 8 Trap charge distribution in the stressed and relaxed states

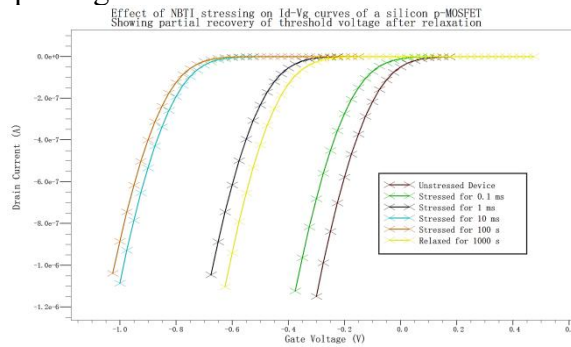


Fig. 9 Effect of NBTI stressing on pmos

It can be seen that the absolute value of the gate leakage current keeps getting larger with the increase of the gate-source voltage at different stress times, and the more serious the NBTI degradation of the PMOS tube. The gate leakage current keeps getting larger as the stress time increases. The increase of the gate source voltage leads to the increase of the electric field strength of the gate oxide layer, and there are a large number of hot holes in the channel inversion of the PMOS tube under the negative gate voltage, and the enhancement of the electric field of the gate oxide layer causes many hot holes to be injected into the gate dielectric layer and then be captured by the trap to generate the oxide charge, which ultimately leads to the exacerbation of the NBTI degradation. The gate leakage current becomes larger with increasing stress time. Therefore, comparing these results with the test results is found to be consistent. The absolute value of saturation leakage source current becomes smaller after NBTI degradation of PMOS tube. As the stress time increases, the NBTI degradation of the PMOS tube becomes more obvious, but the degradation rate gradually becomes slower, and at the later stage of the reaction, the transport of the hydrogen substance is limited to a certain extent, which leads to a gradual decrease of the degradation rate and finally reaches the saturation value. When the stress time increases, the absolute value of the saturation drain-source current decreases, the absolute value of the threshold voltage increases, and the transconductance decreases. For PMOSFETs, when the Fermi energy

level is close to the valence band (P-channel transistor inverse), the donor interface state trap is positively charged, and the receiver interface state trap is neutral, and the interface state trap will cause a negative threshold voltage drift. The degradation is partially recoverable, and the degradation after 1000 s of relaxation is better than that after 100 s of stress. This is due to the structural relaxation of some traps back to the precursor state, while some remain in the charged interface (Pb) state.

5. Summary

For the problem that the ultra-wideband electromagnetic pulse on a certain type of anti-tank director fuze all-electronic safety system will cause low missile damage effectiveness, put forward a joint simulation method of the electromagnetic pulse irradiation effect of the ultra-wideband pulse on a certain type of anti-tank missile fuze electromagnetic pulse. Compared with the traditional analysis method, the method of this paper has the following advantages:

(1) The UWB pulse, which is denser in high-frequency energy, is more likely to cause interference to small-size fuzes. The method in this paper combines the advantages of different electromagnetic effect analysis methods, and can effectively analyse the irradiation effect of UWB electromagnetic pulse on the electromagnetic pulse of a certain type of anti-tank missile fuze.

(2) Based on the existing fuze model and circuit, using different simulation software from the establishment of the structural model of the fuze shell that meets the requirements, the use of joint simulation methods, the electrical and thermal effects of the ultra-wideband EMP to establish a complete simulation system from the 'field' to the 'device'. A complete simulation system from 'field' to 'device' is established for the electrical and thermal effects of ultra-wideband EMP.

(3) The simulation results generated by this method can be mirrored with the EMP injection test. The use of the joint simulation method in a comprehensive assessment of the fuse in the ultra-wideband EMP irradiation capacity at the same time, but also to accurately understand the fuse system in the sensitive devices, resulting in fuse failure, damage to the underlying causes and the future anti-tank missile fuse electromagnetic protection design provides a reference role.

References

- [1] CHEN Kaibai, GAO Min, ZHOU Xiaodong, CHENG Cheng. Front-door coupling effect of ultra-wideband electromagnetic pulse for FMCW fuze[J]. *Systems Engineering and Electronics*, 2020, 42(3): 528-535.
- [2] Zhang wei, Du zhengwei. Simulation of irradiation effects of high power microwave on PCB circuits[J]. *High Power Laser and Particle Beams*, 2011, 23.
- [3] ZHENG Fuquan, LOU Wenzhong, YANG Jingang, FENG Hengzhen. Simulation and Evaluation Method of Fuze Electromagnetic Pulse Coupling Effect[J]. *Journal Of Detection & Control*, 2020, 42(01): 21-28.
- [4] Korte S, Camp M, Garbe H. Hardware and software simulation of transient pulse impact on integrated circuits. *Proceedings of International Symposium on the Electromagnetic Compatibility*, Chicago, IL, United states, 2005.
- [5] L.W. Regate waiting, paragraph translation. *Nuclear electromagnetic pulse radiation and protection technology*. Beijing: National Defense Industry Press, 1980.
- [6] Egawa H. Avalanche Characteristics and Failure Mechanism of High Voltage Diodes[J]. *IEEE Trans on Electron Devices*, 1966, 13(11): 754-758.
- [7] Ren Xinrong, Chai Changchun, Ma Zhenyang. Electrothermal characteristics of second breakdown in diodes under the EMP stress [J]. *JOURNAL. OF XIDIAN UNIVERSITY*, 2013, 40 (02): 36-42.
- [8] Li Bingham, Yu Taoyi, Hua Xiaochun. Study on the Improvement of Negative Bias Temperature Instability in PMOS [J]. *Application Of IC*, 2023, 40(04): 48-51. DOI: 10.19339/j.issn.1674-2583.2023.04.016.